JACS
JOURNAL OF THE AMERICAN CHEMICAL SOCIETY
Article
pubs.acs.org/JACS

Molecular Structure and Chemical Property of a Divalent Metallofullerene Yb@C_2(13)-C_{84}

Wenjun Zhang,[†] Mitsuaki Suzuki,[‡,§] Yunpeng Xie,[†] Lipiao Bao,[†] Wenting Cai,[†] Zdenek Slanina,[‡] Shigeru Nagase,[∥] Ming Xu,*[,†] Takeshi Akasaka,[†,‡,§] and Xing Lu*[,†]

[†]State Key Laboratory of Materials Processing and Die & Mold Technology, School of Materials Science and Engineering, Huazhong University of Science and Technology (HUST), Wuhan 430074, China

[‡]Life Science Center of Tsukuba Advanced Research Alliance, University of Tsukuba, Tsukuba, Ibaraki 305-8577, Japan

[§]Foundation for Advancement of International Science, Tsukuba, Ibaraki 305-0821, Japan

[∥]Fukui Institute for Fundamental Chemistry, Kyoto University, Takano-Nishihiraki-cho 34-4, Sakyo-ku, Kyoto 606-8103, Japan

Supporting Information

ABSTRACT: Endohedral metallofullerenes (EMFs) encapsulating divalent metal ions have received limited attention because of their low production yields. Here, we report the results of structural determination and chemical functionalization of a typical divalent metallofullerene, Yb@C_{84}(II). Single-crystal X-ray crystallographic studies of Yb@C_{84}/Ni^{II}(OEP) cocrystals (OEP is the dianion of octaethylporphyrin) unambiguously established the chiral C_2(13)-C_{84} cage structure and revealed multiple sites for Yb^{2+}, indicating a moving metal ion inside the cage. The chemical property of Yb@C_2(13)-C_{84} was probed with the electrophillic adamantylidene carbene (**1**). Three monoadduct isomers were isolated and characterized. Crystallographic results of the major isomer (**2b**) revealed that, although the cycloaddition breaks a [5,6]-bond on the cage, Yb^{2+} is localized under a hexagonal ring distant from the sites of addition. Thus, it is proved that the dynamic motion of the divalent metal ion in Yb@C_{84} has been effectively halted by exohedral functionalization. Spectroscopic results show that the electronic property of Yb@C_2(13)-C_{84} is pertained in the derivatives, although the addend exerts a mild reduction effect on the electrochemical behavior of the EMF. Computational works demonstrated that addition of **1** to Yb@C_2(13)-C_{84} is mainly driven by releasing the local strains of cage carbons rather than charge recombination, which is always prominent to the affinity of typical trivalent EMFs such as M@C_{2v}(9)-C_{82} (M = Sc, Y, La, Ce, Gd) toward **1**. Accordingly, it is speculated that the chemical behaviors of divalent EMFs more likely resemble those of empty fullerenes because both are closed-shell compounds, but they differ from those of trivalent EMFs, which have open-shell electronic configurations instead.

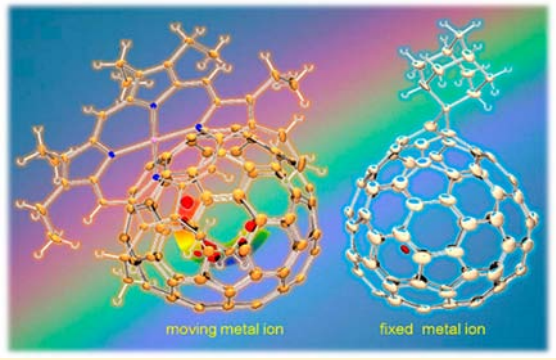

INTRODUCTION

Endohedral metallofullerenes (EMFs) are novel hybrid molecules resulting from endohedral metal-doping of fullerenes with metallic species. It is now acknowledged that not only pure metal atoms but many kinds of otherwise unstable metallic clusters could also be encapsulated inside fullerenes.[1] Among these species identified so far, mono-EMFs, that is, fullerenes encapsulating only one metal atom, are viewed as the simplest prototypes for elucidating the role that the metal atom plays in controlling the inherent properties of the cage carbons and the whole EMF molecules.[2]

One intriguing feature of EMFs is the intramolecular electron transfer from the internal metallic species to the surrounding carbon cage. For mono-EMFs, two different types are identified according to the number of transferred electrons: trivalent EMFs contain a metal atom that transfers three electrons to the cage, while divalent EMFs are these compounds with a metal atom donating only two electrons. An interesting fact is that divalent EMFs are much less produced than the trivalent analogues even using the most effective arc-discharge method; accordingly, divalent EMFs have not been investigated intensively.[3] Recently, several divalent EMFs have been obtained, and their molecular structures have been unambiguously elucidated with single-crystal X-ray diffraction (XRD) crystallography. Such compounds include Ba@C_{74},[4] Yb@C_{2n} ($2n$ = 80, 82),[5] Sm@C_{2n} ($2n$ = 80, 82, 84, 90, 92, 94),[6] and M@C_{94} (M = Ca, Sm, Tm).[7] It is noteworthy that the cage structures of these divalent EMFs are normally different from those of the corresponding empty fullerenes or the trivalent EMFs, confirming a templating effect of the internal metal ion on the cage structures.[8]

Although the structural determination of divalent EMFs continues to develop, their chemistry is in the early infancy.

Received: May 25, 2013
Published: August 1, 2013

   dx.doi.org/10.1021/ja405223t | J. Am. Chem. Soc. 2013, 135, 12730−12735

Chemical transformations reported so far have mainly focused on such readily available species as trivalent EMFs (e.g., La@C_{82}), di-EMFs (e.g., $La_2@C_{80}$), and cluster EMFs (e.g., $Sc_3N@C_{80}$).[1,2] Many meaningful results relating to the mutual influences between the encaged metal ions (e.g., position and electronic configuration) and the cage carbon atoms have been obtained.[9] However, the research of the chemistry of divalent EMFs has lagged far behind. Very recently, the chemical properties of Yb@C_{74} and Yb@C_{84} were investigated with a disilirane reagent.[10] It was surprising to find that these divalent EMFs are more inert than other EMFs explored so far. However, no pure isomers of the silylated derivatives have been obtained due to the many regioisomers formed and scarceness of the samples as well. Fortunately, a recent survey on the chemical property of Yb@C_{80} using 2-adamantane-2,3-[3*H*]-diazirine (AdN_2, **1**) demonstrated a high regioselectivity by affording exclusively one monoadduct isomer, which has been systematically characterized with a collection of experimental and computational means.[11] On the basis of concrete X-ray crystallographic and computational results, it was proposed that the chemical behaviors of divalent EMFs resemble those of empty fullerenes, rather than those of corresponding trivalent analogues.

In this Article, we present the first single-crystal X-ray crystallographic results of a typical divalent EMF, that is, Yb@C_{84}(II), which was cocrystallized with Ni(OEP) (OEP is the dianion of octaethylporphyrin); then we describe the chemical functionalization results of this EMF with **1**. XRD crystallography revealed that the divalent Yb^{2+} cation prefers a dynamic motion inside the cage in pristine Yb@C_2(13)-C_{84}, but it is fixed in the derivative (**2b**). Moreover, this is the first report on the X-ray structure of a functionalized EMF with a C_{84} cage.

EXPERIMENTAL SECTION

High-performance liquid chromatography (HPLC) was conducted on an LC-908 machine (Japan Analytical Industry Co., Ltd.) using toluene as mobile phase. Matrix-assisted laser desorption/ionization time-of-flight (MALDI-TOF) mass spectrometry was measured on a BIFLEX III spectrometer (Bruker, Germany) using 1,1,4,4-tetraphenyl-1,3-butadiene as matrix. Vis−NIR spectra were measured on a UV 3150 spectrometer (Shimadzu, Japan) in toluene. Differential pulse voltammetry (DPV) was measured in 1,2-dichlorobenzene (*o*-DCB) with 0.05 M $(n\text{-Bu})_4NPF_6$ at a Pt working electrode with a potentiostat/galvanostat workstation (BAS CW-50).

Synthesis, isolation, and spectroscopic characterization of Yb@C_{84}(II) were reported previously.[8] Cocrystals of Yb@C_{84}/Ni(OEP) were obtained by layering a benzene solution of Ni(OEP) on top of a CS_2 solution of the endohedral over 2 weeks at 273 K. X-ray diffraction measurements were performed at 90 K on a Bruker AXS machine equipped with an Apex II CCD camera. The multiscan method was used for absorption corrections. The structure was solved with a direct method and was refined using SHELEXS 97.[12]

Calculations were conducted with the Gaussian 09 program package.[13] Geometries were optimized on the basis of the corresponding X-ray results at the B3LYP/6-31G*∼SDD level[14] with the SDD basis set for Yb and the 6-31G* basis for C.

Functionalization of Yb@C_{84}. A sealed Pyrex tube containing 40 mL of toluene solution of Yb@C_2(13)-C_{84} (ca. 2 mg) and an excess amount (ca. 30-fold) of 2-adamantane-2,3-[3*H*]-diazirine (AdN_2, **1**) was degassed with the freeze−pump−thaw method for three cycles. Next, the mixture was irradiated with an ultrahigh pressure mercury-arc lamp (cutoff < 350 nm) at room temperature (Scheme 1).[15] The reaction was traced with HPLC, and the profiles are shown in Figure S1, Supporting Information. Unexpectedly, bis-adducts were formed simultaneously with mono-adducts in the beginning of the reaction. As a result, the reaction was terminated after 10-min irradiation when multiple adducts appeared. The reaction mixture then was concentrated and filtrated for subsequent HPLC separation. As shown in Figure 1, three monoadduct isomers (**2a**, **2b**, **2c**) with a relative abundance ratio of 1:6:1 were isolated. Accordingly, **2b** is the major adduct, whereas **2a** and **2c** are minor isomers. Purities of the three isomers were estimated as higher than 99% with both HPLC and mass spectrometry (Figures S2 and S3, Supporting Information).

Scheme 1. Photochemical Reaction between Yb@C_{84}(II) and 1

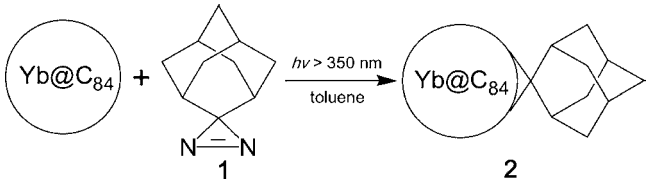

Black crystalline rods of the major isomer (**2b**) suitable for X-ray diffraction measurements were grown from *o*-DCB/hexane in a glass tube (i.d. = 7.0 mm) at 273 K over 10 days. X-ray intensity data were collected at 120 K on a Rigaku DSC imaging plate system by using Si-monochromated synchrotron radiation (λ = 1.00000 Å) at beamline BL-1A of Photon Factory, High-Energy Accelerator Research Organization.

RESULTS AND DISCUSSION

The EMF under study is the most abundant Yb@C_{84} isomer, that is, Yb@C_{84}(II). Previous ^{13}C NMR studies suggested that the cage has C_2 symmetry. Computational works revealed that among the five C_2-symmetric C_{84} isomers that comply with the isolated pentagon rule, C_2(13)-C_{84} is the most stable one after encapsulating an ytterbium atom with two-electron transfer.[8] However, no information about the metal location inside the cage is deducible from the NMR results. Thus, we performed cocrystallization of this EMF with Ni(OEP) using an interfacial diffusion method. Fortunately, a piece of black crystal of Yb@C_{84}/Ni(OEP) allows accurate X-ray crystallographic studies about the details of the molecular structure. This crystal falls in the monoclinic *C*2/*m* space group, as commonly encountered in many analogues EMF/Ni(OEP) systems, which contains two halves of the fullerene cage and a symmetry-related Ni(OEP) molecule.[16] Accordingly, an intact cage is obtainable by combining one-half of the cage with the mirror image of the other, both having an occupancy value of 0.50. Because the C_2(13)-C_{84} cage is chiral, the two cage orientations are actually enantiomers. Inside the cage, up to nine metal sites are distinguished. Their occupancy values are 0.27 for Yb1, 0.09 for Yb2, 0.03 for Yb3, 0.03 for Yb4, 0.02 for Yb5, 0.02 for Yb6, 0.02 for Yb7, 0.01 for Yb8, and 0.01 for Yb9, respectively (Figure S4, Supporting Information). Because none of them resides at the symmetric plane, nine additional metal sites are generated by symmetric operation. This result suggests that the divalent Yb^{2+} prefers a motional behavior inside the cage even at 90 K. This situation is different from that found for Yb@C_{2v}(3)-C_{80} where Yb^{2+} is fixed beneath a hexagonal ring apart from the 2-fold cage axis.[5b] The motion of Yb^{2+} is considered as a result of the relatively "round" cage shape and the evenly distributed negative charges over the cage. Figure 2 shows the molecular structure of Yb@C_{84}/Ni(OEP) with the major metal site (Yb1 of 0.27 occupancy) encapsulated inside one cage orientation. On the basis of the X-ray results, our calculations confirm that the configuration shown in Figure 2 is the most stable structure for Yb@C_2(13)-C_{84}, while the other possible configuration by encapsulating Yb1 inside the mirror image of the cage does not

dx.doi.org/10.1021/ja405223t | J. Am. Chem. Soc. 2013, 135, 12730−12735

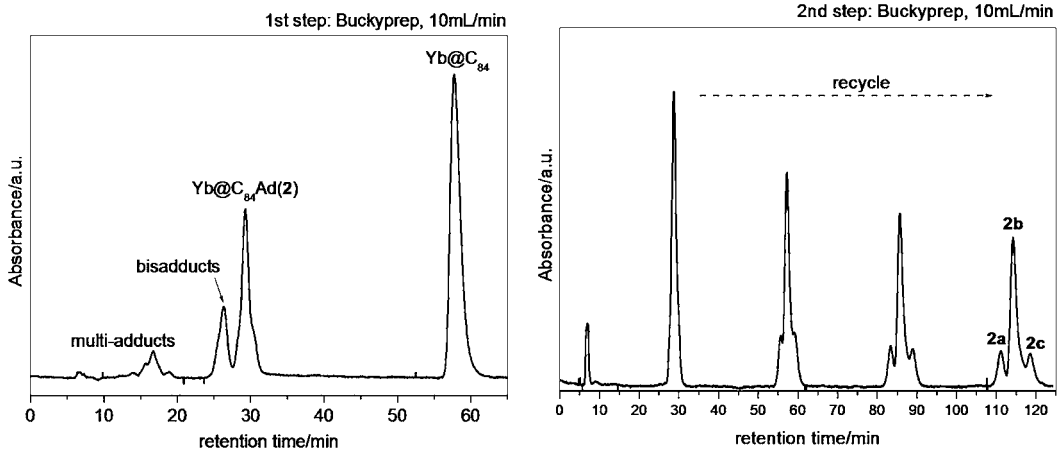

Figure 1. Two-step HPLC separation of Yb@C_2(13)-C_{80}Ad (**2a**, **2b**, **2c**) with a Buckyprep column (10 mL/min toluene flow; 330 nm detection wavelength; room temperature).

Figure 2. X-ray structure of Yb@C_2(13)-C_{84}/Ni(OEP) containing only the major metal site (Yb1, 0.27 occupancy) showing thermal ellipsoid at the 30% probability level. For clarity, solvent molecules, minor metal sites, and the other cage orientation are omitted. Connections between Yb1 and the nearest cage carbons are indicated with dashed bonds.

correspond to an energy minimum.[17] The shortest distance between Ni and a cage carbon is 2.807 Å, featuring a $\pi-\pi$ interaction between the fullerene and Ni(OEP). Yb1 is located beneath a hexagonal ring away from the C_2-axis. The distances between Yb1 and the cage carbons consisting of the adjacent cage hexagon range from 2.630 to 2.745 Å.

The chemical property of Yb@C_2(13)-C_{84} was studied using adamantylidene carbene (**1**), which has been frequently employed to investigate the chemical behaviors of EMFs.[15] Three monoadduct isomers were isolated with HPLC, and the molecular structure of the major isomer (**2b**) was firmly determined by single-crystal X-ray crystallography.

Formation of a 1:1 adduct was initially confirmed by MALDI-TOF mass spectrometry. Because the spectra of the three isomers are nearly identical, only that of **2b** is shown in Figure 3a, and the others are put in Figure S3, Supporting Information. The spectrum displays only one molecular ion peak at m/z 1316, concretely establishing the molecular formula as Yb@C_{84}($C_{10}H_{14}$). The absence of any fragmentation peak indicates the high stability of the derivative under laser irradiation.

Electronic structures of the derivatives (**2a**, **2b**, **2c**) were characterized with absorption spectroscopy. The spectra are shown in Figure 3b together with that of pristine Yb@C_2(13)-C_{84} for comparison. Yb@C_2(13)-C_{84} displays distinct peaks at 510, 600, 630, 780, and 1020 nm with an onset at 1230 nm, corresponding to a medium optical bandgap (1.01 eV). The spectra of **2b** and **2c** largely resemble that of Yb@C_2(13)-C_{84},

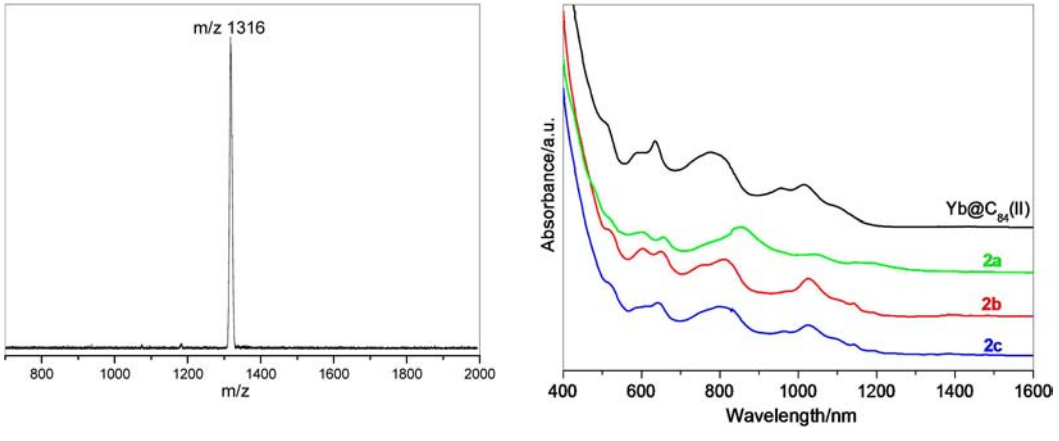

Figure 3. (a) MALDI-TOF mass spectrum of Yb@C_2(13)-C_{84}Ad (**2b**). (b) Vis–NIR spectra of Yb@C_2(13)-C_{84} and **2a**, **2b**, **2c** in toluene.

dx.doi.org/10.1021/ja405223t | J. Am. Chem. Soc. 2013, 135, 12730–12735

although the spectrum of **2a** shows slight alternations in the region between 800 and 1000 nm. According to the existing knowledge that open-cage derivatives of EMFs generally retain the same number of π-electrons as pristine EMFs and thus keep the electronic properties largely, it is conclusive that **2a**−**2c** all have open-cage structures.[18]

Molecular structure of the major isomer (**2b**) was concretely determined with single-crystal XRD crystallography. It is noteworthy that this is the first report on the X-ray structure of any EMF-derivative with a fullerene cage larger than C_{82}. The structure suffers from disorder. The Ad group features two disordered positions, which are shifted slightly by 0.3−1.2 Å. Each disordered Ad group links with two cage orientations, which are enantiomers. Thus, four disordered cage orientations are detected in total. Within the cage, four metal sites are also distinguished. According to their spatial relationships, it is reasonable to assign each metal site to a respective cage orientation. Figure 4 illustrates the X-ray structure of **2b** with a major metal site encapsulated in the major cage. Addition of Ad breaks a [5,6]-bond junction, resulting in a fulleroid structure of **2b**. Surprisingly but interestingly, the metal ion is not trapped inside the cavity where the [5,6]-bond is cleaved, but it sits steadily under a hexagonal ring distant from the sites of addition. The distances between Yb1 and the cage carbons consisting of the adjacent hexagon range from 2.437 to 2.608 Å, which are slightly shorter than the corresponding values found in Yb@C_{84}/Ni(OEP) cocrystals. Such strong metal−cage interactions may account for the stationary location of the metal ion in **2b**. The placement of the Yb^{2+} ion found here is completely different from the situations observed in the corresponding Ad-derivatives of other mono-EMFs reported previously, such as M@C_{82}Ad (M = Sc, Y, La, Ce, Gd), in which the metal ion is always trapped inside the cavity provided by bond-breaking upon Ad addition.[15]

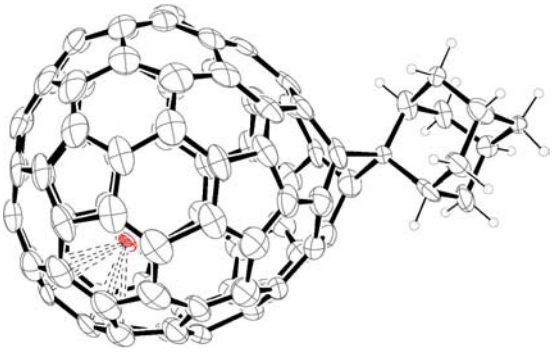

Figure 4. X-ray structure of Yb@C_2(13)-C_{84}Ad (**2**) with thermal ellipsoid set at the 30% probability level. Only the major cage orientation and the pairing metal site are shown. For clarity, solvent molecules, the other cage orientations, and minor metal sites are omitted. Connections between Yb and the nearest hexagon cage carbons are indicated with dashed bonds.

In contrast, the addition pattern in **2b** is similar to that observed for Yb@C_{80}Ad, where the metal ion is distant from the sites of addition. It has been proposed that **1** acts as an electrophile when reacting with EMFs. Accordingly, the negative charges on the cage carbons are primary driving forces for their affinity to **1**. This is particularly true for M@C_{82}-type (M = Sc, Y, La, Ce, and Ge) EMFs because in these compounds the excessive negative charges are mainly localized on these cage carbons interacting strongly with the internal trivalent cation.[15] However, for divalent EMFs, the charge densities are more evenly distributed over the cage, and resultantly the local strain of each cage carbon becomes more prominent for its reactivity toward **1**. The pyramidalization angles from the p-orbital axis vector (POAV) analysis are useful indexes of the local strains on the cage carbons. As shown in Figure S5, Supporting Information, the carbons at the sites of addition in **2b** bear relatively high POAV angles, but they have very low negative charge densities. These results are consistent with those observed for Yb@C_{80}Ad: the carbons at the sites of addition are distant from the internal Yb^{2+} ion, and they have relatively low charge density values but high local strains.

The electrochemical properties of **2b** were characterized with differential pulse voltammetry (DPV), but observation of the

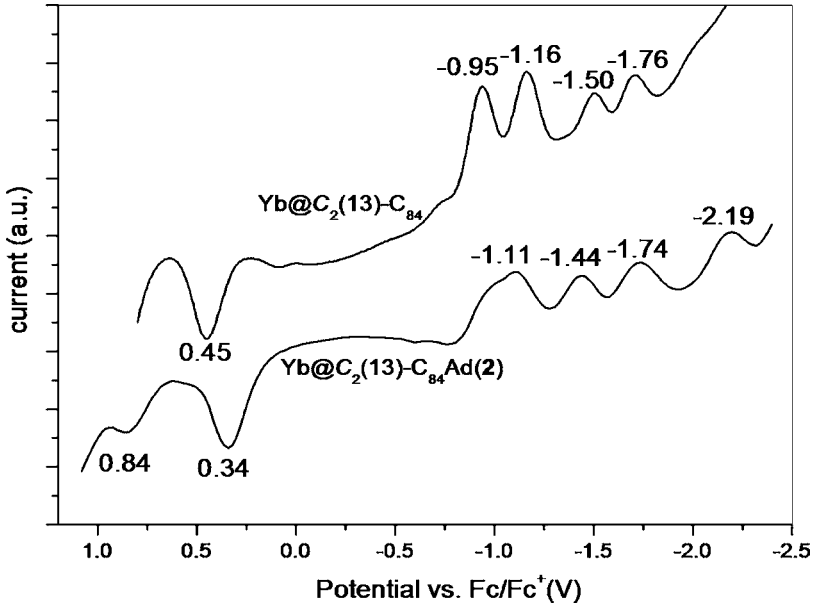

Figure 5. DPV diagrams of Yb@C_2(13)-C_{84} and **2b**.

dx.doi.org/10.1021/ja405223t | J. Am. Chem. Soc. 2013, 135, 12730−12735

Table 1. Redox Potentials[a] (V vs Fc/Fc^+) of Yb@C_2(13)-C_{84} and 2b

compound	$^{ox}E_2$	$^{ox}E_1$	$^{red}E_1$	$^{red}E_2$	$^{red}E_3$	$^{red}E_4$
Yb@C_2(13)-C_{84}[b]		0.45	−0.95	−1.16	−1.50	−1.76
2b	0.84	0.34	−1.11	−1.44	−1.74	−2.19

[a]DPV values on a Pt-working electrode in 1,2-dichlorobenzene. [b]Reference 8.

redox processes of **2a** and **2c** was unsuccessful because of the scarcity of the samples. As shown in Figure 5, four peaks in the anodic region and two oxidation waves are observed for **2b**. This property resembles largely the electrochemical behavior of pristine Yb@C_2(13)-C_{84}.[8] However, the redox potentials of **2b** are cathodically shifted by 0.11−0.43 V in comparison with the corresponding values of Yb@C_2(13)-C_{84}, confirming an electron-donating ability of the Ad group (Table 1).

CONCLUSION

A typical divalent metallofullerene, Yb@C_{84}(II), has been systematically investigated, focusing on its molecular structure and chemical property. X-ray crystallographic results of the cocrystal of Yb@C_{84}/Ni(OEP) reveal that the divalent Yb^{2+} ion prefers a dynamic motion inside the chiral C_2(13)-C_{84} cage by featuring multiple metal sites. A carbene reagent (**1**) was utilized to probe the chemical property of this EMF. X-ray results of the most abundant monoadduct isomer (**2b**) confirm a [5,6]-open structure, which is the first X-ray result of any EMF-derivative bearing a cage larger than C_{82}. It is interesting to find that the dynamic motion of the metal ion in Yb@C_2(13)-C_{84} is completely stopped in **2b**, although the metal is not trapped inside the cavity provided by bond cleavage. Our results present new features about the metal location and metal−cage interaction in these less-explored species, which has improved our knowledge about the structures and inherent properties of divalent EMFs, and help to establish the art of reactivity control of different molecules at the atomic level.

ASSOCIATED CONTENT

Supporting Information

Chromatographic and spectroscopic results of the derivatives, and X-ray data of Yb@C_2(13)-C_{84} and **2b** in CIF format. This material is available free of charge via the Internet at http://pubs.acs.org.

AUTHOR INFORMATION

Corresponding Author

lux@hust.edu.cn

Notes

The authors declare no competing financial interest.

ACKNOWLEDGMENTS

Financial support from The National Thousand Talents Program of China, NSFC (21171061, 21271067), KAKENHI from MEXT Japan (20108001 pi-space, 202455006, 24350019, 20036008, 20038007, and 22000009), and The Strategic Japanese-Spanish Cooperative Program funded by JST and MICINN is acknowledged.

REFERENCES

(1) For typical reviews in the past five years, see: (a) Lu, X.; Akasaka, T.; Nagase, S. *Acc. Chem. Res.* **2013**, *46*, 1627−1635. (b) Popov, A.; Yang, S.; Dunsch, L. *Chem. Rev.* **2013**, DOI: 10.1021/cr300297r. (c) Xie, Y. P.; Lu, X.; Akasaka, T.; Nagase, S. *Polyhedron* **2013**, *52*, 3−9. (d) Akasaka, T.; Lu, X. *Chem. Rec.* **2012**, *12*, 256−269. (e) Lu, X.; Feng, L.; Akasaka, T.; Nagase, S. *Chem. Soc. Rev.* **2012**, *41*, 7723−7760. (f) Rodriguez-Fortea, A.; Balch, A. L.; Poblet, J. M. *Chem. Soc. Rev.* **2011**, *40*, 3551−3563. (g) Osuna, S.; Swart, M.; Sola, M. *Phys. Chem. Chem. Phys.* **2011**, *13*, 3585−3603. (h) Yamada, M.; Akasaka, T.; Nagase, S. *Acc. Chem. Res.* **2010**, *43*, 92−102. (i) Chaur, M. N.; Melin, F.; Ortiz, A. L.; Echegoyen, L. *Angew. Chem., Int. Ed.* **2009**, *48*, 7514−7538.

(2) (a) Lu, X.; Akasaka, T.; Nagase, S. *Chem. Commun.* **2011**, *47*, 5942−5957. (b) Maeda, Y.; Tsuchiya, T.; Lu, X.; Takano, Y.; Akasaka, T.; Nagase, S. *Nanoscale* **2011**, *3*, 2421−2429.

(3) (a) Lian, Y. F.; Shi, Z. J.; Zhou, X. H.; Gu, Z. N. *Chem. Mater.* **2004**, *16*, 1704−1714. (b) Huang, H. J.; Yang, S. H. *J. Phys. Chem. B* **1998**, *102*, 10196−10200.

(4) Reich, A.; Panthofer, M.; Modrow, H.; Wedig, U.; Jansen, M. *J. Am. Chem. Soc.* **2004**, *126*, 14428−14429.

(5) (a) Suzuki, M.; Slanina, Z.; Mizorogi, N.; Lu, X.; Nagase, S.; Olmstead, M. M.; Balch, A. L.; Akasaka, T. *J. Am. Chem. Soc.* **2012**, *134*, 18772−18778. (b) Lu, X.; Lian, Y.; Beavers, C. M.; Mizorogi, N.; Slanina, Z.; Nagase, S.; Akasaka, T. *J. Am. Chem. Soc.* **2011**, *133*, 10772−10775.

(6) (a) Yang, H.; Wang, Z. M.; Jin, H. X.; Hong, B.; Liu, Z. Y.; Beavers, C. M.; Olmstead, M. M.; Balch, A. L. *Inorg. Chem.* **2013**, *52*, 1275−1284. (b) Yang, H.; Jin, H. X.; Wang, X. Q.; Liu, Z. Y.; Yu, M. L.; Zhao, F. K.; Mercado, B. Q.; Olmstead, M. M.; Balch, A. L. *J. Am. Chem. Soc.* **2012**, *134*, 14127−14136. (c) Yang, H.; Yu, M.; Jin, H.; Liu, Z.; Yao, M.; Liu, B.; Olmstead, M. M.; Balch, A. L. *J. Am. Chem. Soc.* **2012**, *134*, 5331−5338. (d) Jin, H. X.; Yang, H.; Yu, M. L.; Liu, Z. Y.; Beavers, C. M.; Olmstead, M. H.; Balch, A. L. *J. Am. Chem. Soc.* **2012**, *134*, 10933−10941. (e) Yang, H.; Jin, H. X.; Zhen, H. Y.; Wang, Z. M.; Liu, Z. Y.; Beavers, C. M.; Mercado, B. Q.; Olmstead, M. M.; Balch, A. L. *J. Am. Chem. Soc.* **2011**, *133*, 6299−6306.

(7) Che, Y. L.; Yang, H.; Wang, Z. M.; Jin, H. X.; Liu, Z. Y.; Lu, C. X.; Zuo, T. M.; Dorn, H. C.; Beavers, C. M.; Olmstead, M. M.; Balch, A. L. *Inorg. Chem.* **2009**, *48*, 6004−6010.

(8) Lu, X.; Slanina, Z.; Akasaka, T.; Tsuchiya, T.; Mizorogi, N.; Nagase, S. *J. Am. Chem. Soc.* **2010**, *132*, 5896−5905.

(9) (a) Shustova, N. B.; Chen, Y. S.; Mackey, M. A.; Coumbe, C. E.; Phillips, J. P.; Stevenson, S.; Popov, A. A.; Boltalina, O. V.; Strauss, S. H. *J. Am. Chem. Soc.* **2009**, *131*, 17630−17637. (b) Yamada, M.; Someya, C.; Wakahara, T.; Tsuchiya, T.; Maeda, Y.; Akasaka, T.; Yoza, K.; Horn, E.; Liu, M. T. H.; Mizorogi, N.; Nagase, S. *J. Am. Chem. Soc.* **2008**, *130*, 1171−1176. (c) Cardona, C. M.; Kitaygorodskiy, A.; Echegoyen, L. *J. Am. Chem. Soc.* **2005**, *127*, 10448−10453.

(10) Ruan, J.; Xie, Y.; Cai, W.; Slanina, Z.; Mizorogi, N.; Nagase, S.; Akasaka, T.; Lu, X. *Fullerenes, Nanotubes, Carbon Nanostruct.* **2013**, DOI: 10.1080/1536383X.2013.794344.

(11) Xie, Y.; Suzuki, M.; Cai, W.; Mizorogi, N.; Nagase, S.; Akasaka, T.; Lu, X. *Angew. Chem., Int. Ed.* **2013**, *52*, 5142−5145.

(12) Sheldrick, G. M. *Acta Crystallogr.* **2008**, *A64*, 112−122.

(13) Frisch, M. J.; Trucks, G. W.; Schlegel, H. B.; Scuseria, G. E.; Robb, M. A.; Cheeseman, J. R.; Scalmani, G.; Barone, V.; Mennucci, B.; Petersson, G. A.; Nakatsuji, H.; Caricato, M.; Li, X.; Hratchian, H. P.; Izmaylov, A. F.; Bloino, J.; Zheng, G.; Sonnenberg, J. L.; Hada, M.; Ehara, M.; Toyota, K.; Fukuda, R.; Hasegawa, J.; Ishida, M.; Nakajima, T.; Honda, Y.; Kitao, O.; Nakai, H.; Vreven, T.; Montgomery, J. A.; Peralta, Jr., J. E.; Ogliaro, F.; Bearpark, M.; Heyd, J. J.; Brothers, E.; Kudin, K. N.; Staroverov, V. N.; Kobayashi, R.; Normand, J.; Raghavachari, K.; Rendell, A.; Burant, J. C.; Iyengar, S. S.; Tomasi, J.; Cossi, M.; Rega, N.; Millam, J. M.; Klene, M.; Knox, J. E.; Cross, J. B.; Bakken, V.; Adamo, C.; Jaramillo, J.; Gomperts, R.; Stratmann, R. E.; Yazyev, O.; Austin, A. J.; Cammi, R.; Pomelli, C.; Ochterski, J. W.; Martin, R. L.; Morokuma, K.; Zakrzewski, V. G.; Voth, G. A.; Salvador,

P.; Dannenberg, J. J.; Dapprich, S.; Daniels, A. D.; Farkas, O.; Foresman, J. B.; Ortiz, J. V.; Cioslowski, J.; Fox, D. J. *Gaussian 09*, revision C.01; Gaussian, Inc.: Wallingford, CT, 2010.

(14) (a) Becke, A. D. *Phys. Rev. A* **1988**, *38*, 3098−3100. (b) Becke, A. D. *J. Chem. Phys.* **1993**, *98*, 5648−5652. (c) Lee, C.; Yang, W.; Parr, R. G. *Phys. Rev. B* **1988**, *37*, 785−789. (d) Cundari, T. R.; Stevens, W. J. *J. Chem. Phys.* **1993**, *98*, 5555−5565. (e) Cao, X. Y.; Dolg, M. *J. Mol. Struct. (THEOCHEM)* **2002**, *581*, 139−147. (f) Hay, P. J.; Wadt, W. R. *J. Chem. Phys.* **1985**, *82*, 299−310. (g) Hehre, W. J.; Ditchfield, R.; Pople, J. A. *J. Chem. Phys.* **1972**, *56*, 2257−2261. (h) Wolinski, K.; Hilton, J. F.; Pulay, P. *J. Am. Chem. Soc.* **1990**, *112*, 8251−8260. (i) Sun, G. Y.; Kertesz, M. *J. Phys. Chem. A* **2000**, *104*, 7398−7403.

(15) (a) Hachiya, M.; Nikawa, H.; Mizorogi, N.; Tsuchiya, T.; Lu, X.; Akasaka, T. *J. Am. Chem. Soc.* **2012**, *134*, 15550−15555. (b) Lu, X.; Nikawa, H.; Feng, L.; Tsuchiya, T.; Maeda, Y.; Akasaka, T.; Mizorogi, N.; Slanina, Z.; Nagase, S. *J. Am. Chem. Soc.* **2009**, *131*, 12066−12067. (c) Akasaka, T.; Kono, T.; Takematsu, Y.; Nikawa, H.; Nakahodo, T.; Wakahara, T.; Ishitsuka, M. O.; Tsuchiya, T.; Maeda, Y.; Liu, M. T. H.; Yoza, K.; Kato, T.; Yamamoto, K.; Mizorogi, N.; Slanina, Z.; Nagase, S. *J. Am. Chem. Soc.* **2008**, *130*, 12840−12841. (d) Maeda, Y.; Matsunaga, Y.; Wakahara, T.; Takahashi, S.; Tsuchiya, T.; Ishitsuka, M. O.; Hasegawa, T.; Akasaka, T.; Liu, M. T. H.; Kokura, K.; Horn, E.; Yoza, K.; Kato, T.; Okubo, S.; Kobayashi, K.; Nagase, S.; Yamamoto, K. *J. Am. Chem. Soc.* **2004**, *126*, 6858−6859.

(16) (a) Olmstead, M. H.; de Bettencourt-Dias, A.; Duchamp, J. C.; Stevenson, S.; Marciu, D.; Dorn, H. C.; Balch, A. L. *Angew. Chem., Int. Ed.* **2001**, *40*, 1223−1225. (b) Zuo, T. M.; Beavers, C. M.; Duchamp, J. C.; Campbell, A.; Dorn, H. C.; Olmstead, M. M.; Balch, A. L. *J. Am. Chem. Soc.* **2007**, *129*, 2035−2043.

(17) Suzuki, M.; Lu, X.; Sato, S.; Nikawa, H.; Mizorogi, N.; Slanina, Z.; Tsuchiya, T.; Nagase, S.; Akasaka, T. *Inorg. Chem.* **2012**, *51*, 5270−5273.

(18) (a) Lukoyanova, O.; Cardona, C. M.; Rivera, J.; Lugo-Morales, L. Z.; Chancellor, C. J.; Olmstead, M. M.; Rodriguez-Fortea, A.; Poblet, J. M.; Balch, A. L.; Echegoyen, L. *J. Am. Chem. Soc.* **2007**, *129*, 10423−10430. (b) Li, X. F.; Fan, L. Z.; Liu, D. F.; Sung, H. H. Y.; Williams, I. D.; Yang, S.; Tan, K.; Lu, X. *J. Am. Chem. Soc.* **2007**, *129*, 10636−10637. (c) Lu, X.; Nikawa, H.; Nakahodo, T.; Tsuchiya, T.; Ishitsuka, M. O.; Maeda, Y.; Akasaka, T.; Toki, M.; Sawa, H.; Slanina, Z.; Mizorogi, N.; Nagase, S. *J. Am. Chem. Soc.* **2008**, *130*, 9129−9136. (d) Lu, X.; Nikawa, H.; Tsuchiya, T.; Maeda, Y.; Ishitsuka, M. O.; Akasaka, T.; Toki, M.; Sawa, H.; Slanina, Z.; Mizorogi, N.; Nagase, S. *Angew. Chem., Int. Ed.* **2008**, *47*, 8642−8645. (e) Shu, C. Y.; Xu, W.; Slebodnick, C.; Champion, H.; Fu, W. J.; Reid, J. E.; Azurmendi, H.; Wang, C. R.; Harich, K.; Dorn, H. C.; Gibson, H. W. *Org. Lett.* **2009**, *11*, 1753−1756. (f) Li, F.-F.; Rodriguez-Fortea, A.; Poblet, J. M.; Echegoyen, L. *J. Am. Chem. Soc.* **2011**, *133*, 2760−2765.